Supporting Information

Porous, pH Responsive, and Reusable Hydrogel Beads of Bovine Serum Albumin_Au Hybrid as Smart Nanofactories for the Removal of Organic and Inorganic Pollutants from Water: A Detailed Demonstration by Spectroscopy and Microscopy

Aekta Upadhyay and Chebrolu Pulla Rao*

Bioinorganic Laboratory, Department of Chemistry, Indian Institute of Technology Bombay, Powai, Mumbai – 400 076, India, E-mail: cprao@iitb.ac.in

Contents

SI 01: **Synthesis of BSA_Au NCs**: In 20 ml vial, 100 mg/ml BSA was dissolved in 5 ml water. To this solution, five ml of (50 mM) $HAuCl_4.3H_2O$ was dropwise added under stirring at 450 rpm. The solution was kept under stirring at room temperature for 10 minutes and thereafter dropwise addition of 1 M NaOH was done to make the pH of the solution 12. The solution was stirred for another 48 hours at RT to form a dark red colour solution. The solution was stored at 4°C and characterised.

SI 02: Adsorption kinetics: Different terms used

$q = \frac{C_0 - C_t}{M} \times V \ (\frac{mg}{g})$	**Adsorption capacity (*q*)**
$\log(q_e - q_t) = \log(q_e) - \frac{k_1 t}{2.303}$	**Pseudo first order rate kinetics**
$\frac{t}{q_t} = \frac{1}{K_2 q_e^2} + \frac{t}{q_e}$	**Pseudo second order rate kinetics**
$\frac{C_e}{q_e} = \frac{1}{b q_m} + \frac{C_e}{q_m}$	**Langmuir isotherm**
$ln\ q_e = ln\ k_f + \ ln \frac{C_e}{n}$	**Freundlich isotherm**

SI 03: Photograph of BSA, BSA_Au NCs and BSA_Au beads under visible and UV light

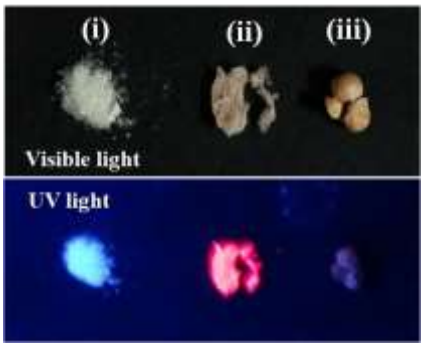

Figure S1: Photograph of (i) only BSA, (ii) lyophilised BSA_Au NC and (iii) lyophilised *Bead$_a$* under visible and UV light.

SI 04: TGA of *Bead*$_a$ and *Bead*$_b$

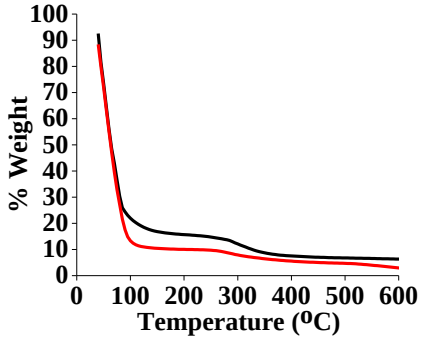

Figure S2: TGA of *Bead*$_a$ (Black) and *Bead*$_b$ (Red).

SI 05: Pore size distribution plot of *Bead*$_a$ and *Bead*$_b$

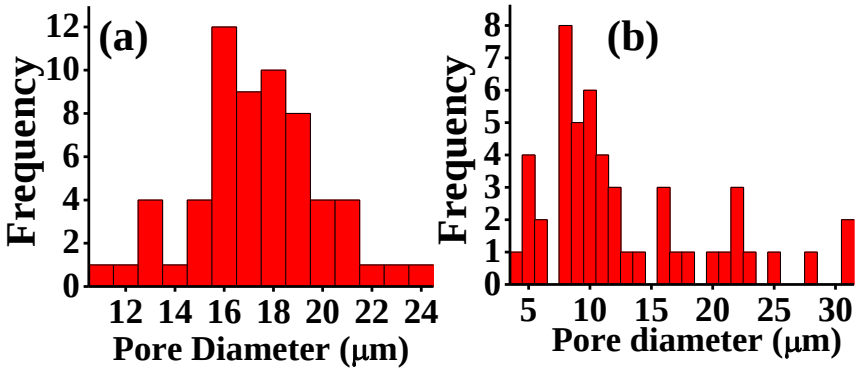

Figure S3: Pore size distribution plot of (a) *Bead*$_a$ and (b) *Bead*$_b$ calculated by imageJ software from SEM micrograph.

SI 06: Mapping of different elements present in lyophilised *Bead*$_a$ by SEM

Figure S4: Mapping of different elements present in lyophilised *Bead*$_a$ by SEM

SI 07: Mapping of elements present in *Bead*$_a$ by STEM

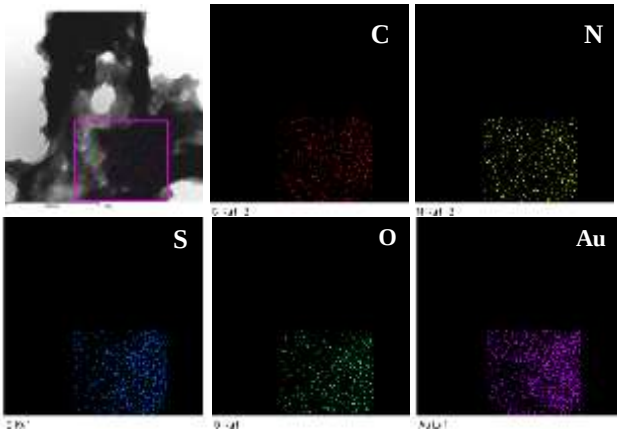

Figure S5: Mapping of elements present in *Bead*$_a$ by STEM.

SI 08: Time dependent UV-Visible spectra of supernatant solution of dyes upon incubation with *Bead*$_a$.

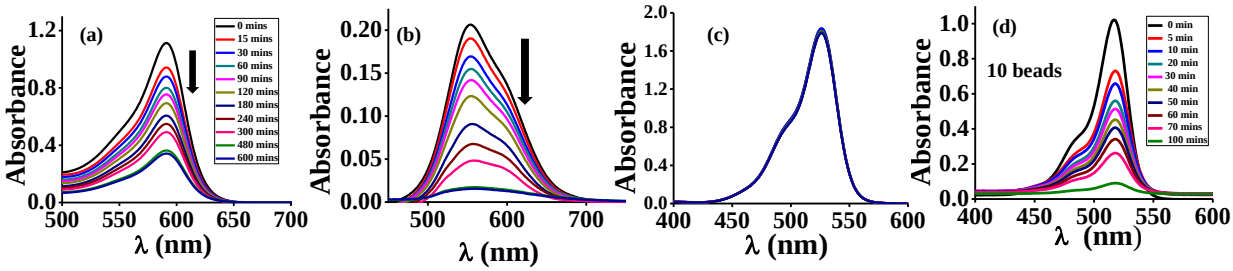

Figure S6: UV Visible spectrum of (a) BB, (b) CBB and (c) R6G when 1 bead is used and (d) EY when 10 beads are used as adsorbent.

SI 09: Table showing the adsorption kinetic parameters by *Bead*$_a$.

Dyes	First order			Second order		
	R^2	K_1	q_{cal} (mg/g)	R^2	K_2	q_{cal} (mg/g)
EY	0.96	4.6×10^{-3}	127.46	0.97	8.6×10^{-5}	175.43
BB	0.938	6.9×10^{-3}	168.15	0.978	5×10^{-5}	194.93
CBB	0.876	9.6×10^{-3}	328.1	0.95	1.4×10^{-5}	313.47

Table S1: R^2, K_1, K_2 and q_{cal} for *Bead*$_a$ adsorbed dyes (EY, BB and CBB).

SI 10: Kinetics and isotherm fitting for *Bead*$_a$@EY.

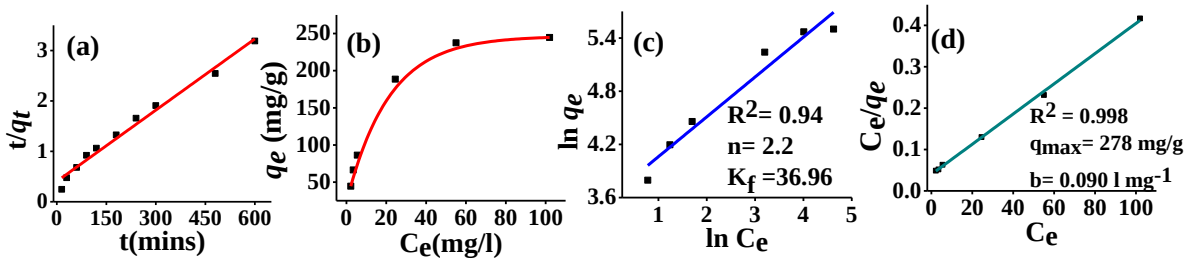

Figure S7: (a) Pseudo second order fit for *Bead*$_a$@EY. (b) Plot of q_e versus C_e for adsorption of EY by *Bead*$_a$. (c) Freundlich and (d) Langmuir isotherms fit for adsorption of EY by *Bead*$_a$.

SI 11: Time dependent adsorption spectra of R6G and MB upon incubation by *Bead*$_b$

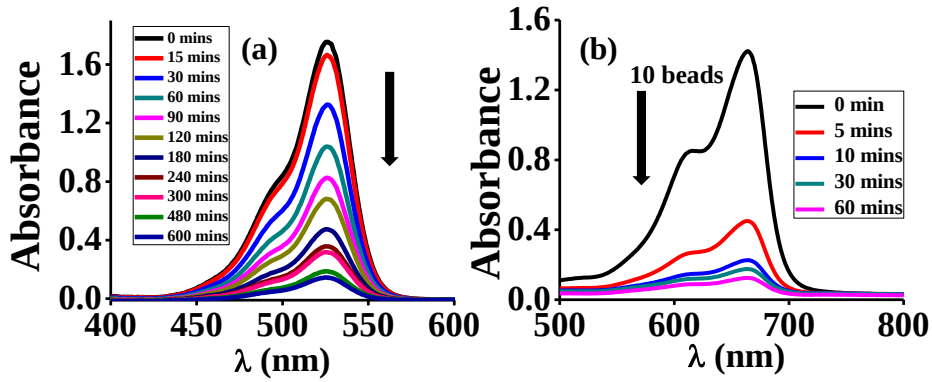

Figure S8: UV-Visible spectrum of supernatant of (a) R6G with respect to time when incubated with one *Bead*$_b$ and (b) MB when incubated with 10 beads.

SI 12: Adsorption kinetics parameters for Bead$_b$@ MB and Bead$_b$@R6G.

Dyes	First order			Second order		
	R^2	K_1	q_{cal} (mg/g)	R^2	K_2	q_{cal} (mg/g)
MB	0.98	6.6×10^{-3}	184.92	0.998	3.6×10^{-5}	333
R6G	0.987	7.6×10^{-3}	171.85	0.988	3.6×10^{-5}	227

Tabe S2: R^2, K_1, K_2 and q_{cal} for *Bead*$_b$ @ MB and *Bead*$_b$ @ R6G

SI 13: Langmuir and Freundlich isotherm fitting for *Bead*$_b$ @ MB.

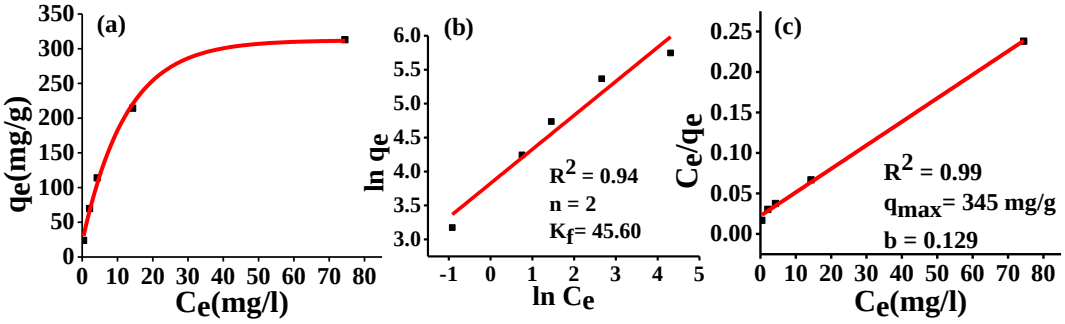

Figure S9: (a) Plot of q_e versus C_e for adsorption of MB by *Bead*$_b$. (b) Freundlich and (c) Langmuir isotherms for adsorption of MB by *Bead*$_b$.

SI 14: Desorption of EY and MB from *Bead*$_a$ and *Bead*$_b$ at different temperatures

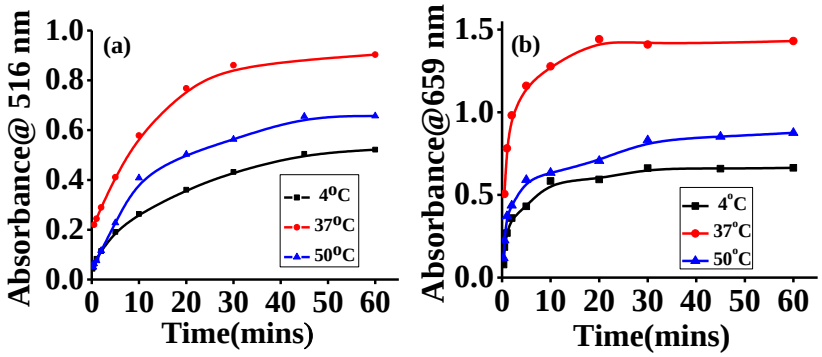

Figure S10: Plot of λ_{max} of corresponding dye versus time taken for desorption at different temperature in case of (a) EY (from *Bead*$_a$) and (b) MB (from *Bead*$_b$).

SI 15: UV-Vis spectra of EY and MB before and after passing through column set-up.

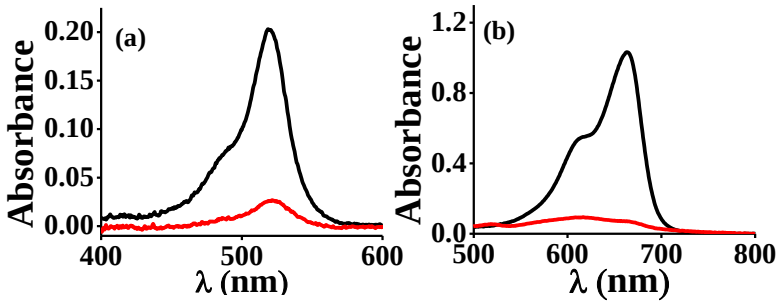

Figure S11: UV-Vis spectra of (a) EY and (b) MB before (Black line) and after (Red line) being adsorbed by beads.

SI 16: Maximum adsorption capacity of Pb^{2+}, Cd^{2+} and Hg^{2+} by *Bead*$_b$

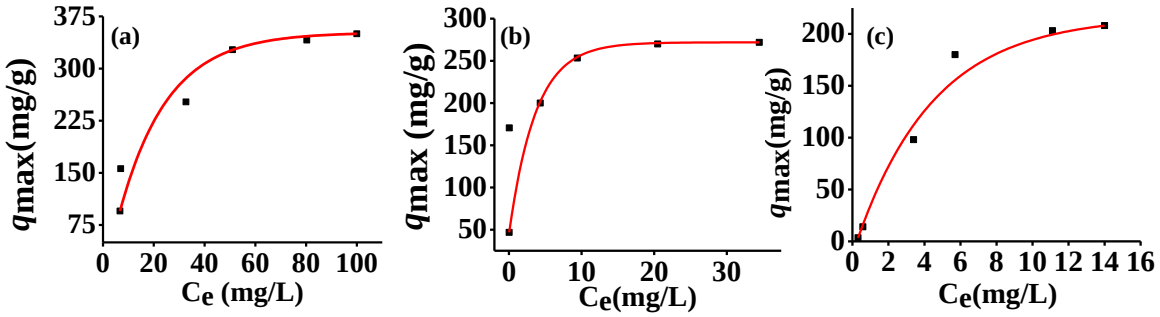

Figure S12: Plot of q_{max} versus C_e for (a) Cd^{2+}, (b) Pb^{2+} and (c) Hg^{2+}

SI 17: Maximum adsorption capacity of $KMnO_4$, K_2PdCl_4 and $HAuCl_4$ by *Bead*$_a$

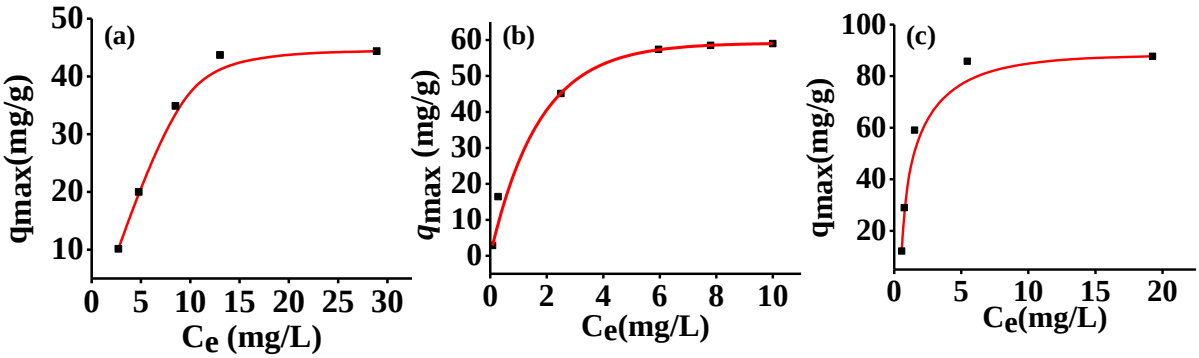

Figure S13: Plot of q_{max} versus C_e for (a) $KMnO_4$, (b) K_2PdCl_4 and (c) $HAuCl_4$